Modal Gating of Human $Ca_V2.1$ (P/Q-type) Calcium Channels: II. The b Mode and Reversible Uncoupling of Inactivation

Tommaso Fellin, Siro Luvisetto, Michele Spagnolo, and Daniela Pietrobon

Department of Biomedical Sciences and Consiglio Nazionale delle Ricerche Institute of Neuroscience, University of Padova, 35121 Padova, Italy

ABSTRACT The single channel gating properties of human $Ca_V2.1$ (P/Q-type) calcium channels were investigated with cell-attached patch-clamp recordings on HEK293 cells stably expressing these calcium channels. Human $Ca_V2.1$ channels showed a complex modal gating, which is described in this and the preceding paper (Luvisetto, S., T. Fellin, M. Spagnolo, B. Hivert, P.F. Brust, M.M. Harpold, K.A. Stauderman, M.E. Williams, and D. Pietrobon. 2004. *J. Gen. Physiol.* 124:445–461). Here, we report the characterization of the so-called b gating mode. A $Ca_V2.1$ channel in the b gating mode shows a bell-shaped voltage dependence of the open probability, and a characteristic low open probability at high positive voltages, that decreases with increasing voltage, as a consequence of both shorter mean open time and longer mean closed time. Reversible transitions of single human $Ca_V2.1$ channels between the b gating mode and the mode of gating in which the channel shows the usual voltage dependence of the open probability (nb gating mode) were much more frequent (time scale of seconds) than those between the slow and fast gating modes (time scale of minutes; Luvisetto et al., 2004), and occurred independently of whether the channel was in the fast or slow mode. We show that the b gating mode produces reversible uncoupling of inactivation in human $Ca_V2.1$ channels. In fact, a $Ca_V2.1$ channel in the b gating mode does not inactivate during long pulses at high positive voltages, where the same channel in both fast-nb and slow-nb gating modes inactivates relatively rapidly. Moreover, a $Ca_V2.1$ channel in the b gating mode shows a larger availability to open than in the nb gating modes. Regulation of the complex modal gating of human $Ca_V2.1$ channels could be a potent and versatile mechanism for the modulation of synaptic strength and plasticity as well as of neuronal excitability and other postsynaptic Ca^{2+}-dependent processes.

KEY WORDS: Ca^{2+} channel • gating mode • synaptic transmission • familial hemiplegic migraine • channelopathy

INTRODUCTION

Ca^{2+} influx through $Ca_V2.1$ (P/Q-type) calcium channels plays a central role in controlling neurotransmitter release in the brain (Dunlap et al., 1995; Mintz et al., 1995; Wu et al., 1999; Qian and Noebels, 2001). $Ca_V2.1$ channels are also involved in regulating neural and cortical network excitability, synaptic integration, and gene expression (Bayliss et al., 1997; Magee et al., 1998; Pineda et al., 1998; Sutton et al., 1999; Mori et al., 2000; van den Maagdenberg et al., 2004). The time course and amplitude of Ca^{2+} influx through Ca_V channels in response to physiological electrical activity is determined by their single channel gating and permeation properties. These properties are then crucial in determining the time course and magnitude of the various Ca^{2+}-dependent processes controlled by $Ca_V2.1$ channels. The single channel study reported in the preceding paper (Luvisetto et al., 2004) revealed a complex modal gating of human $Ca_V2.1$ channels; single channels can display two modes of gating characterized by different latencies to first opening and different mean closed times, different voltage dependence of the open probability, different kinetics of inactivation, and different voltage dependence of steady-state inactivation. Different latencies to first opening and different open probabilities can alter the timing and the magnitude of action potential–evoked Ca^{2+} influx, and can profoundly affect both the timing and magnitude of neurotransmission controlled by $Ca_V2.1$ channels (Borst and Sakmann, 1998; Sabatini and Regehr, 1999). Different properties of inactivation can substantially alter Ca^{2+} influx in response to repetitive firing waveforms (Liu et al., 2003).

Most of the single channel recordings in Luvisetto et al. (2004) were done at voltages ~30 mV lower than those attained at the peak of action potentials recorded in neurons (taking into account the difference in surface potential due to the high divalent ion concentration used in single channel recordings to allow resolution of single channel gating events; c.f. Tottene et al., 2002). Therefore, it seemed interesting to examine the gating properties of the channels at higher voltages. This study revealed frequent switching of

Address correspondence to Daniela Pietrobon, Dept. of Biomedical Sciences, University of Padova, Viale G. Colombo, 3 35121 Padova, Italy. Fax: 39-049-8276049; email: daniela.pietrobon@unipd.it

Abbreviation used in this paper: HEK, human embryonic kidney.

J. Gen. Physiol. © The Rockefeller University Press • 0022-1295/2004/11/463/12 $8.00
Volume 124 November 2004 463–474
http://www.jgp.org/cgi/doi/10.1085/jgp.200409035

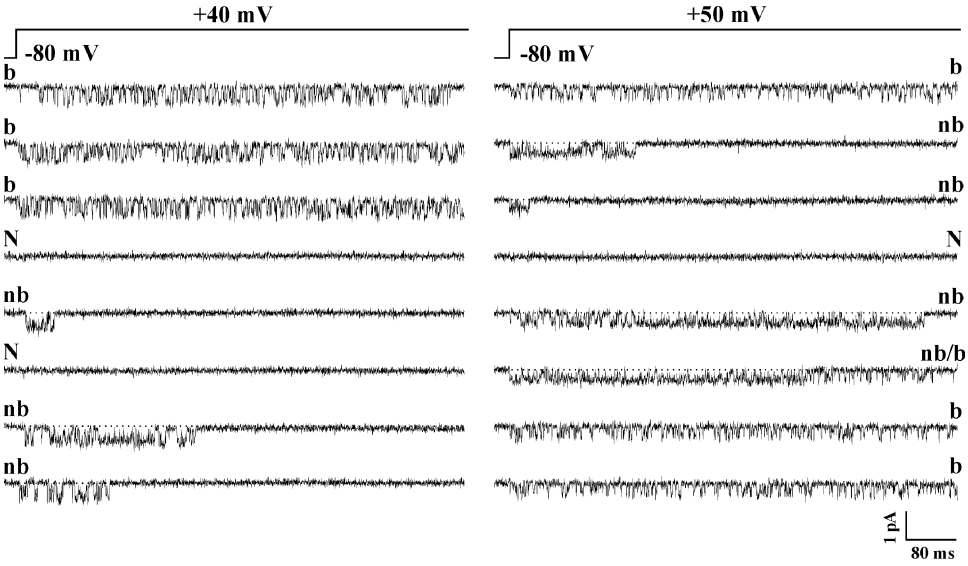

FIGURE 1. Reversible switching of a single human $Ca_V2.1$ channel to a noninactivating mode of gating with low open probability at +40 and +50 mV: the b mode. Cell-attached single channel patch-clamp recordings, with 90 mM Ba^{2+} as charge carrier, from HEK293 cells stably coexpressing human $\alpha_{1A\text{-}2}$, β_{1b}, and $\alpha_{2b}\delta$-1 subunits. Consecutive traces at +40 mV (left) and +50 mV (right) from a patch containing a single $Ca_V2.1$ channel are shown. Labeling of traces: b indicates channel activity with low open probability (b gating mode); nb indicates channel activity with the high open probability expected during periods of activity at high voltages (nb gating mode); N indicates lack of activity (null). Depolarizations were 720 ms long and were delivered every 4 s from holding potentials of −80 mV. Records were sampled and filtered at 5 and 1 kHz, respectively.

single $Ca_V2.1$ channels to an additional mode of gating (the b mode) that is described in this paper. The b gating mode is characterized by the virtual absence of channel inactivation and by a bell-shaped voltage dependence of the open probability, which determines a characteristic low open probability at high positive voltages, decreasing with increasing voltage. We show that the b gating mode produces reversible uncoupling of inactivation in human $Ca_V2.1$ channels.

MATERIALS AND METHODS

Single channel patch-clamp recordings were performed on human embryonic kidney HEK293 cells (American Type Culture Collection, CRL-1533) stably transfected with cDNA constructs encoding the human $Ca_V2.1\alpha_1$ ($\alpha_{1A\text{-}2}$), $\alpha_{2b}\delta$-1, and β_{1b} (A68-90 cell line), as in Luvisetto et al. (2004), or on HEK293 cells transiently transfected with the same cDNAs. In the latter case, CD4 expression plasmids were included to permit the identification of transfected cells as previously described (Hans et al., 1999). In both cases, cells were incubated at 28°C for 12–24 h before electrophysiological measurements (Hans et al., 1999).

All single channel recordings were obtained in cell-attached configuration. The pipette solution contained (in mM) 90 $BaCl_2$, 10 TEA-Cl, 15 CsCl, 10 HEPES (pH 7.4 with TEA-OH). The bath solution contained (in mM) 140 K-gluconate, 5 EGTA, 35 L-glucose, 10 HEPES (pH 7.4 with KOH). The high-potassium bath solution was used to zero the membrane potential outside the patch. Liquid junction potential at the pipette tip was +12 mV and this value should be subtracted from all voltages to obtain correct values of membrane potentials.

Linear leak and capacitative currents were digitally subtracted from all records used for analysis. Single channel open probabilities, activation curves, and open and closed time histograms were obtained as in Luvisetto et al. (2004). All values are given as mean ± SEM.

RESULTS

Single channel recordings at +40 and +50 mV (with 90 mM Ba^{2+} as charge carrier) on HEK293 cells, stably coexpressing human $Ca_V2.1\alpha_1$ ($\alpha_{1A\text{-}2}$), β_{1b}, and $\alpha_{2b}\delta$-1 subunits, revealed that a $Ca_V2.1$ channel in either the fast or slow gating mode (Luvisetto et al., 2004) can reversibly and frequently (in the time scale of seconds) switch to a noninactivating gating mode with low open probability, p_o, that we have called b mode. Fig. 1 shows consecutive traces at +40 and +50 mV from a patch containing a single $Ca_V2.1$ channel that alternates between an inactivating mode of gating with the high open probability expected during periods of activity at these high voltages (traces labeled nb) and a noninactivating gating mode with lower p_o, the b mode (traces labeled b). The sixth trace at +50 mV shows a transition to the b mode during the depolarization. Here, and in the following, p_o refers to the open probability during periods of channel activity; it is calculated excluding the last shut time due to channel entering into an inactivated state, and therefore reflects the equilibrium between short-lived open and closed states.

The fraction of time spent by a single $Ca_V2.1$ channel in the b gating mode was very variable from patch to patch (from 0 to 90%). Transitions back and fourth to

the b gating mode were much more frequent than transitions between the slow and fast gating modes (Luvisetto et al., 2004), and occurred independently of whether the channel was in the fast or the slow gating mode. This is shown in Fig. 2, which displays histograms of the open probability measured in individual sweeps at different voltages in patches containing a single channel in either the fast gating mode ($n = 4$, left) or the slow gating mode ($n = 6$, right). The open probability histograms of $Ca_V2.1$ channels in either the fast or the slow gating mode show two peaks at +40 and +50 mV. The peaks at lower p_o reflect the presence of the b gating mode shown in Fig. 1. However, the p_o histograms at +20 and +30 mV show only one peak, in agreement with the lack of evidence for a low-p_o mode at +30 mV (c.f. Luvisetto et al., 2004). The values of the open probabilities at the peak of the gaussian functions, used to fit the histograms, are plotted as a function of voltage in the bottom panels of Fig. 2. Considering the higher-p_o peaks at +40 and +50 mV, the open probability increases with increasing voltage in the usual sigmoidal way, tending toward a maximum value close to 0.6 for both the fast and slow gating modes. Considering the lower-p_o peaks, reflecting the b gating mode, the open probability does not increase and actually tends to decrease with voltage above +40 mV (for both the fast-b and slow-b modes). Indeed, in individual patches, a single channel in the b gating mode showed consistently a lower open probability at +50 mV than at +40 mV (c.f. traces in Fig. 1).

The temporal correlation among sweeps with low-p_o activity (b gating mode) and among those with high-p_o activity (or nb gating mode, as we will call it from now on) in individual single channel patches was studied by constructing contingency tables with the number of pairs of consecutive traces in the four possible combinations (b-b, b-nb, nb-b, and nb-nb), and by performing run analysis (Horn et al., 1984; Nilius, 1988; Plummer and Hess, 1991). A cut-off p_o value of 0.45 was used to classify channel activity in each depolarization at +40 or +50 mV as b or nb mode (c.f. p_o histograms in Fig. 2). Fig. 3 A shows the sequences of sweeps in two single channel patches classified as b, nb, or N (null), and Fig. 3 B shows the corresponding number of pairs of consecutive traces in the four different combinations. The latter were used to calculate the probability that the observed contingency tables arose from random association of traces with b-type and nb-type activity, given the known overall occurrence of each gating pattern during the entire experiments. In the 13 single channel patches examined, the probability of random occurrence assessed by a χ^2 test was less than 0.05 in each patch (<0.001 in seven patches). Run analysis confirmed the nonrandom occurrence of the b gating mode, since it gave z values ranging from 1.82 to 5.75

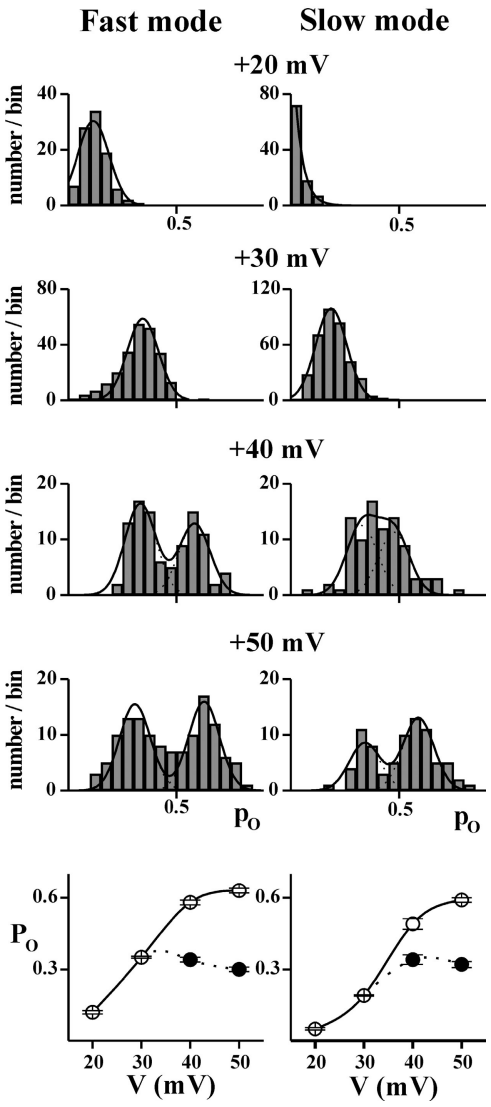

FIGURE 2. Single human $Ca_v2.1$ channels in either the fast or slow gating mode display the b gating mode at +40 and +50 mV. Single channel recordings as in Fig. 1. In each patch, the depolarization voltage was cyclically changed from +10 to +50 mV in 10-mV steps. Histograms of the open probability, p_o, measured in individual sweeps at different voltages in four patches containing a single channel in the fast gating mode (left) and six patches containing a single channel in the slow gating mode (right) are shown. The p_o was measured only in sweeps with activity excluding the last shut time. The classification of the single channel activity as either slow or fast gating mode was based on visual inspection of the gating pattern at +30 mV, on the open and closed time histograms at +30 mV, and on the voltage dependence of the average open probability (Luvisetto et al., 2004). The p_o histograms at +20 and +30 mV were best fitted with a single gaussian function. The histograms at +40 and +50 mV were best fitted with the sum of two Gaussian functions, with a fixed width equal to that best fitting the histogram at +30 mV (slow mode); the peaks at lower p_o reflect the presence of the b gating mode. The values of p_o at the peak of the Gaussian functions are plotted as a function of voltage in the bottom panels; the symbol ● represents the p_o values of the b gating mode at +40 and +50 mV.

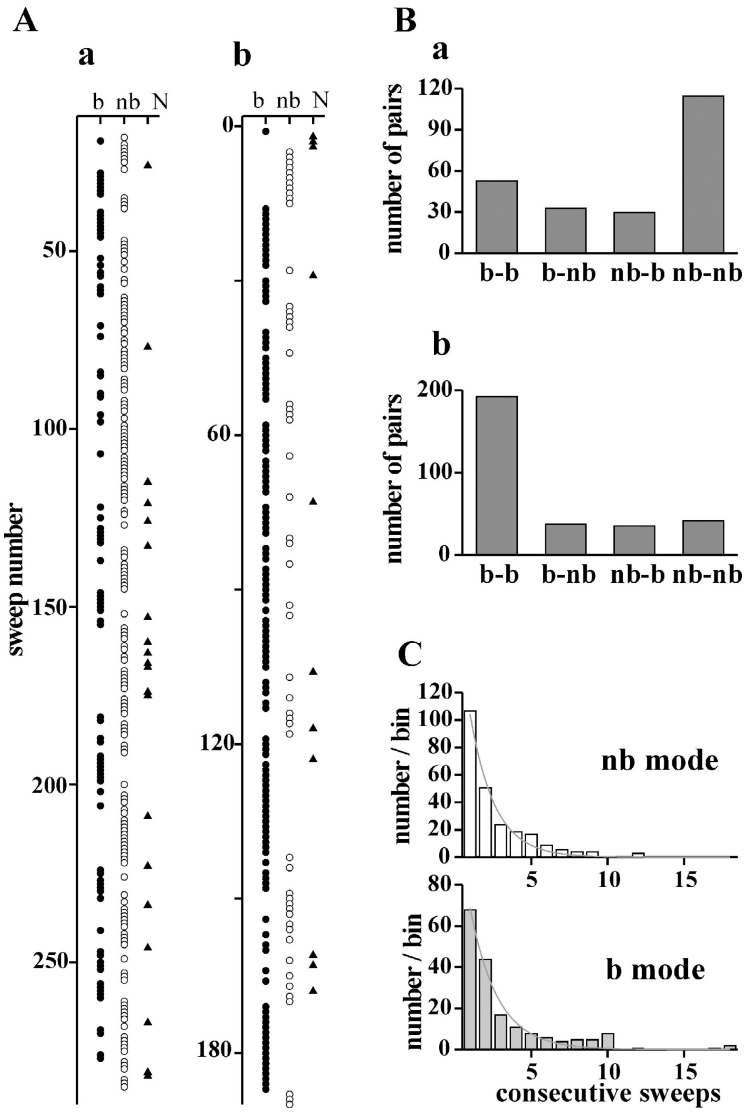

FIGURE 3. Temporal correlation among sweeps with low-p_o (b) and high-p_o (nb) gating patterns and mean lifetime of the b and nb modes. Cell-attached patch-clamp recordings as in Fig. 1 on HEK293 cells stably or transiently coexpressing human $\alpha_{1A\text{-}2}$, β_{1b}, and $\alpha_{2b}\delta$-1 subunits. (A, a and b) Sequences of sweeps in two representative single channel patches, classified as b or nb on the basis of a cut-off p_o value of 0.45 at +50 mV. N represents sweeps without activity (nulls). (B, a and b) Number of pairs of consecutive traces in the four different combinations (b-b, b-nb, nb-b, and nb-nb) in the two single channel patches shown in A, a and b. Pairs containing nulls were not counted. (C) Number of consecutive traces with either b or nb gating mode activity in 13 single channel patches, plotted as histograms with binwidth of one trace. Fitting with a single exponential function gives mean lifetimes of 1.6 traces (6.4 s) for the nb gating mode and 1.8 traces (7.2 s) for the b gating mode. If nulls within a string of sweeps with nb or b mode activity were considered as part of the gating mode, then the mean lifetime of the nb gating mode would increase relative to that of the b mode (compare Fig. 7).

in 11 single channel patches (with number of sweeps ranging from 64 to 327), higher than the minimal value of $z = 1.64$ required to reject randomness at the $P = 0.05$ level (Horn et al., 1984; Nilius, 1988). Thus, the b gating pattern (as well as the nb gating pattern) remains correlated over the duration of the interpulse interval (4 s). To estimate the average lifetimes of the b and nb gating modes, we constructed histograms of the number of consecutive traces in b and nb modes in the different single channel patches (Fig. 3 C). Fit of the histograms with a single exponential function gave mean lifetimes of 1.6 traces (6.4 s) for the nb gating mode and 1.8 traces (7.2 s) for the b gating mode.

In the recordings at +30 mV, there was no evidence of the b gating mode clearly seen at higher voltages (Luvisetto et al., 2004; and c.f. single peak in p_o histograms in Fig. 2). To try to understand this finding, we adopted the double pulse protocol shown in Fig. 4, in which a prepulse to +20 or +30 mV was followed by a short pulse to +50 mV. We could then separate (using the cut-off p_o value of 0.45) the traces in which the channel was in the b gating mode during the short pulse at +50 mV (and presumably also during the prepulse at +30 or +20 mV) from those in which it was in the nb gating mode. As shown by the representative traces in Fig. 4, the single channel activity at +30 mV (and even more at +20 mV) was similar in the b and nb gating modes (compare first two and last two traces at both voltages). Also similar were the open as well as the closed time histograms of the channel in the two gating modes at +30 mV. Indeed, Fig. 4 B shows that the average values of the open and closed time constants of the exponential components best fitting the open and closed time distributions at +30 mV of single $Ca_V2.1$ channels in the fast-nb or the fast-b gating mode were not significantly different. The open probability at +30 mV was also similar in b (0.36 ± 0.03) and nb (0.38 ± 0.05) gating modes. Similar open probabilities (p_o =

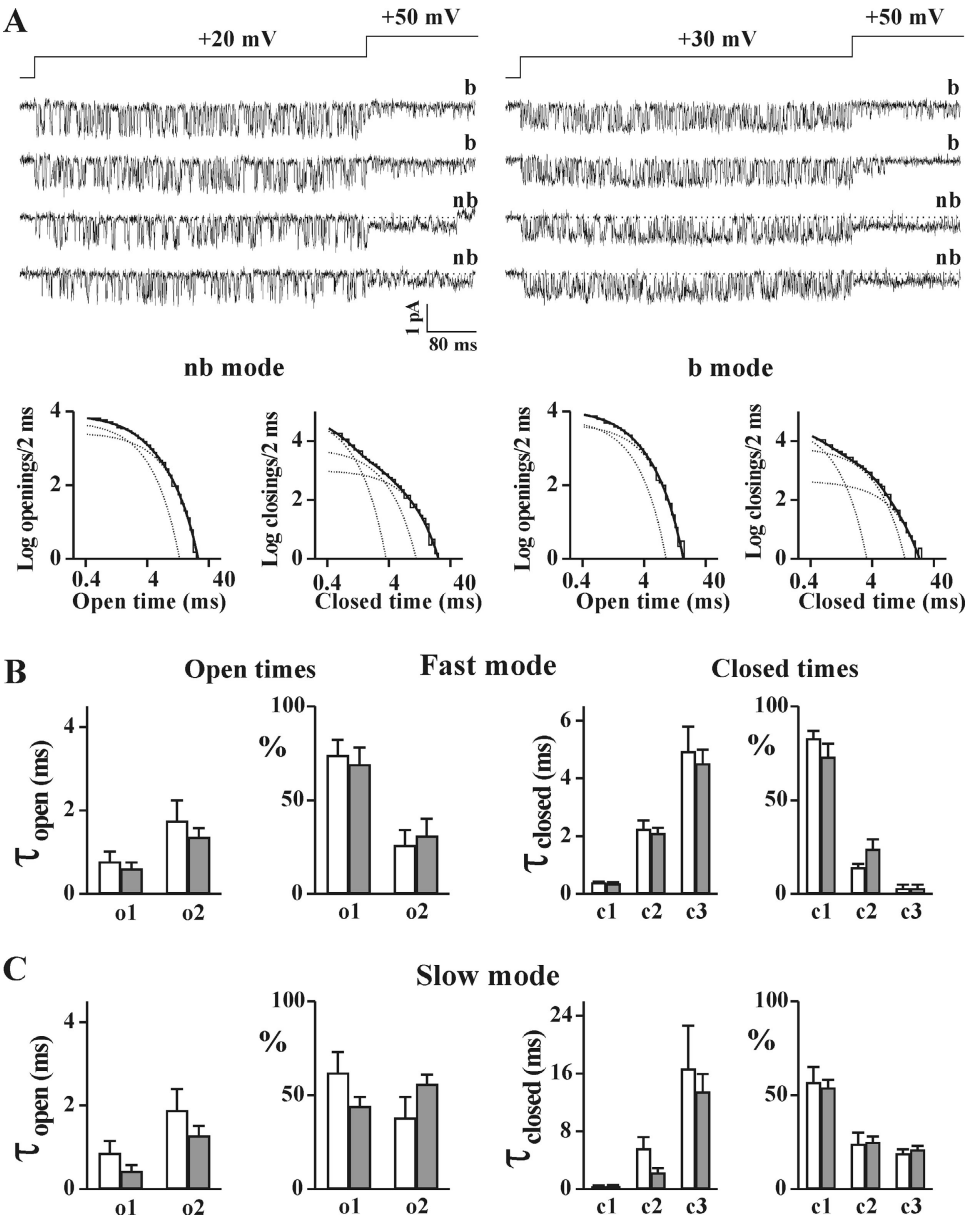

FIGURE 4. At V < +40 mV, a $Ca_V2.1$ channel in the b gating mode has similar open probability and open and closed time distributions than in the nb mode. Cell-attached patch-clamp recordings from single channel patches as in Fig. 3, but with a voltage protocol in which 540-ms-long depolarizations to either 20 or 30 mV were followed by 180-ms-long depolarizations to +50 mV. (A) Representative single channel current traces from a patch containing a single $Ca_V2.1$ channel, which alternates between the nb and b modes of gating, are shown together with log–log plots of the open and closed time distributions at +30 mV, obtained for the nb (left) and the b gating mode (right), after separation of the traces in the two gating modes on the basis of the activity in the short pulse at +50 mV that follows the depolarization at +30 mV. Judging from the activity at +30 mV, the single channel in the patch was in the fast gating mode for the entire period, and, at any given voltage, had a higher open probability than usually found for this gating mode (e.g., the maximal p_o at +50 mV in the nb gating mode was 0.86, to be compared with values of 0.6–0.7 for most of the single channel analyzed), mainly due to unusually long mean open times (Luvisetto et al., 2004). The dark solid line in each plot is the best-fitting sum of exponential components (two for the open times and three for the closed times), each shown as a dotted line (minimum number of components indicated by the maximum likelihood ratio test); time constants for the open times, 1.04 and 2.06 ms (relative areas 41 and 59%) for the b gating mode, and 1.56 and 3.42 ms (relative areas 48 and 52%) for the nb gating mode; time constants for the closed times, 0.31, 1.56, and 3.84 ms (relative areas 50, 42, and 8%) for the b gating mode, and 0.32, 1.29, and 3.7 ms (relative areas 70, 20, and 10%) for the nb mode. Thanks to the unusually long mean open times, this channel showed a small but significant difference in the time constants best fitting the open time distributions for the b and nb gating modes, in contrast with the similar average values shown in B. (B) Time constants (τ_{open} and τ_{closed}) and relative areas (%) of the exponential components best fitting the open and closed time distributions at +30 mV of single $Ca_V2.1$ channels in the fast-nb (empty bar) and the fast-b (gray bar) gating modes. Average values were obtained from four patches containing a single channel in the fast gating mode. (C) Time constants (τ_{open} and τ_{closed}) and relative areas (%) of the exponential components best fitting the open and closed time distributions at +30 mV of single $Ca_V2.1$ channels in the slow-nb (empty bar) and the slow-b (gray bar) gating modes. Average values from three single channel patches.

0.2 ± 0.02 and 0.21 ± 0.04 in the b and nb gating modes, respectively) and similar open and closed time histograms (Fig. 4 C) were obtained also for single channels in the slow-b and slow-nb gating modes. The single peaks at +30 and +20 mV in the p_o histograms of Fig. 2 and the lack of evidence for the b gating mode at +30 mV are then due to the fact that, at V < +40 mV, the open and closed time distributions of a channel in the b and nb gating modes are so similar that the two gating modes become indistinguishable.

Different open and closed time constants for the b and nb gating modes were obtained at + 40 mV (Fig. 5).

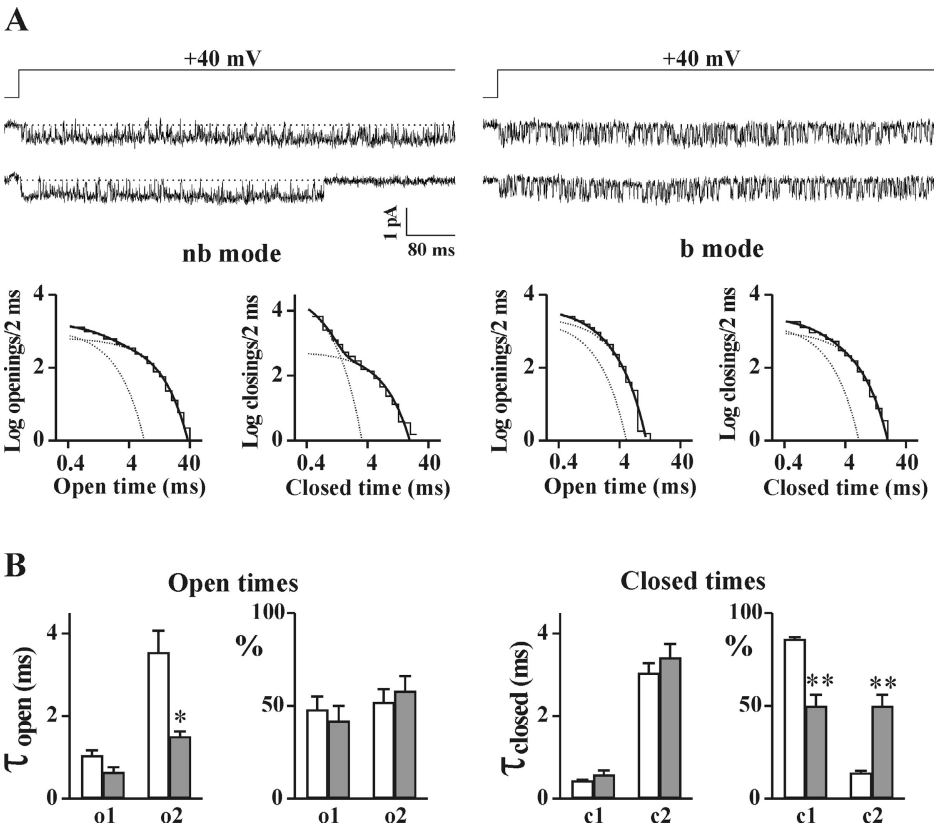

FIGURE 5. At +40 mV, a $Ca_V2.1$ channel in the b gating mode has shorter open times and spends a larger fraction of time in a relatively long closed state than the same channel in the nb mode. Single channel recordings as in Fig. 1. (A) Representative single channel current traces at +40 mV, from a patch containing a single $Ca_V2.1$ channel (same patch as in Fig. 4), which alternates between the nb (left) and the b mode of gating (right), are shown together with the corresponding log–log plots of the open and closed time distributions, obtained after separation of the traces in the two gating modes using a discriminating p_o value of 0.45. Judging from the activity at +30 mV, the single channel in the patch was in the fast gating mode for the entire period. The dark solid line in each plot is the best-fitting sum of two exponential components (each exponential component is shown as a dotted line); time constants of the open times, 1.33 and 5.74 ms (relative areas 30 and 70%) for the nb gating mode and 0.68 and 1.42 ms (relative areas 29 and 71%) for the b mode; time constants of the closed times, 0.30 and 3.13 ms (relative areas 89 and 11%) for the nb gating mode and 0.91 and 2.91 ms (relative areas 33 and 67%) for the b mode. While two exponential components were required by the maximum likelihood test to fit the open times in the nb gating mode, one (τ = 1.24 ms) or two components were equally likely in the b mode. (B) Time constants (τ_{open} and τ_{closed}) and relative areas (%) of the two exponential components best fitting the open and closed time distributions at +40 mV of single $Ca_V2.1$ channels in the nb (empty bar) and the b (gray bar) gating modes. Average values for the nb and b gating modes were obtained from five and four single channel patches, respectively. Statistical significance of difference between paired values using Student's *t* test: *, $P < 0.05$; **, $P < 0.001$.

Fig. 5 shows that the lower p_o at +40 mV of a $Ca_V2.1$ channel in the b gating mode (with respect to that of the same channel in the nb mode) is due to shorter open times and to a larger fraction of time spent in a relatively long closed state. Although the very small unitary current impaired a reliable kinetic analysis at +50 mV, open times in the b mode appeared to further shorten and closed times to further lengthen with increasing voltage. The b gating mode appears then characterized by a bell-shaped voltage dependence of the open probability that reaches its maximum value (~50% the $p_{o,max}$ of the nb gating mode) at 35–40 mV and then tends to decrease (compare Fig. 2) as a consequence of both shorter mean open time and longer mean closed time. These features of the b gating mode seemed consistent with voltage-dependent open channel block by a cytoplasmic positively charged particle, hence the name of blocked mode initially given to the low-p_o gating mode observed at high voltages. However, other properties of $Ca_V2.1$ channels in this gating mode, discussed below, are not expected from a simple block mechanism, and therefore the name b mode seems preferable.

One of these properties is the lack of inactivation of a $Ca_V2.1$ channel in the b mode (Figs. 6 and 7, c.f. also Fig. 1). At +50 mV, a $Ca_V2.1$ channel in the slow-b or the fast-b gating mode does not inactivate during 720 ms, in contrast with the same channel in the slow-nb or fast-nb gating mode (Fig. 6 A). As also shown in Luvisetto et al. (2004), inactivation is faster in the fast-nb than in the slow-nb mode.

The availability of a $Ca_V2.1$ channel in the b mode also appears to differ from that of the same channel in the nb gating mode. In fact, within a string of sweeps with b mode activity, nulls were found much less frequently than in a string of sweeps with nb mode activity (Fig. 7 and its legend, and also Fig. 3). In eight single channel patches, the probability that a sweep with nb mode activity was preceded or followed by a null sweep (174 pairs/754 pairs = 0.23) was more than four times greater than the probability that a sweep with b mode activity was preceded or followed by a null (32/585 pairs = 0.055).

From the average ensemble currents in Fig. 6 B, after scaling on the basis of the fraction of null traces in the

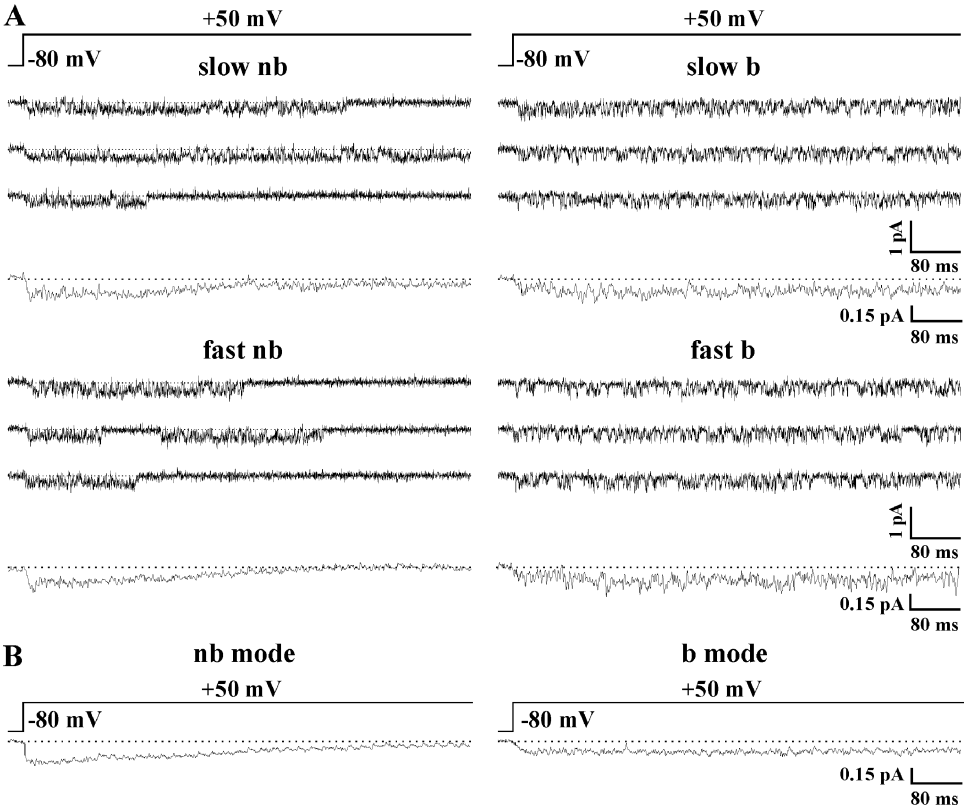

FIGURE 6. A $Ca_V2.1$ channel in the b gating mode does not inactivate, in contrast with the same channel in the nb mode. Single channel recordings as in Fig. 3. (A, top) Representative consecutive current traces at +50 mV and corresponding average ensemble currents (n = 12 and 11 for the nb and b gating mode, respectively) from a patch containing a single channel switching between the nb (left) and the b (right) gating mode. Judging from the gating at +30 mV, the channel was in the slow gating mode. (A, bottom) As above, but from a patch containing a single channel in the fast mode (average ensemble currents, n = 16 and 8 for the nb and b gating mode, respectively). (B) Pooled average single channel ensemble currents at +50 mV (n = 101 and 61 for the nb and b gating mode, respectively), obtained from seven single channel patches (with channels in both fast and slow mode), after separation of the b and nb gating modes using the usual discriminating p_o value of 0.45.

two modes, one can obtain an estimation of the possible impact of b to nb mode switching on the macroscopic current. A population of channels in the (mixed fast and slow) nb gating mode would generate a 1.6 times larger peak current than the same channels in the b mode, but a 0.94 times smaller integrated (over 720 ms) current.

Inactivating and noninactivating gating modes with mean lifetimes similar to those of the b and nb modes of $Ca_V2.1$ channels and with similar differences in channel availability in the two gating modes have been described for native N-type Ca^{2+} channels ($Ca_V2.2$) (Plummer and Hess, 1991). Switching between the two inactivating and noninactivating gating modes produces the so called reversible uncoupling of inactivation of N-type channels. Mean open time and latency to first opening were very similar for single N-type channels in the inactivating and noninactivating gating modes at +20 mV (the only depolarization examined by Plummer and Hess, 1991). Likewise, $Ca_V2.1$ channels have similar open times (Fig. 4) and first latency (not depicted) at +30 (and +20) mV in the b and nb gating modes. We used a double pulse protocol, similar to that shown in Fig. 4, to investigate whether switching between the nb and b gating modes produced reversible uncoupling of inactivation of $Ca_V2.1$ channels at +30 mV, as observed at higher voltages (Fig. 6). The number of traces showing channel inactivation at +30 mV during periods of b mode activity (as inferred from the gating pattern in the short pulse at +50 mV following the prepulse at +30 mV) were compared with those during periods of nb mode activity (Fig. 7). In the representative patch shown in Fig. 7, containing a single $Ca_V2.1$ channel in the fast gating mode, channel inactivation at +30 mV was observed almost exclusively during periods of nb mode activity (compare the channel activity in consecutive sweeps, classified as b, nb, null, and inactivating, in the bottom panel). The probability that an nb sweep was preceded or followed by an inactivating sweep (31/61 pairs = 0.51) was more than three times larger than the probability that a b sweep was preceded or followed by an inactivating sweep (8/50 pairs = 0.16, and in most cases it occurred in correspondence of transitions between the b and nb gating mode). The separate ensemble averages of nb and b traces (Fig. 7) show that at +30 mV, as observed at higher voltages, a $Ca_V2.1$ channel in the b gating mode does not inactivate, in contrast with the clear inactivation displayed by the same channel in the nb gating mode. We therefore conclude that switching between the nb and b gating modes produces reversible uncoupling of inactivation of $Ca_V2.1$ channels. Note that, given the slow inactivation of $Ca_V2.1$ channels in the inactivating nb gating mode (considerably slower at both

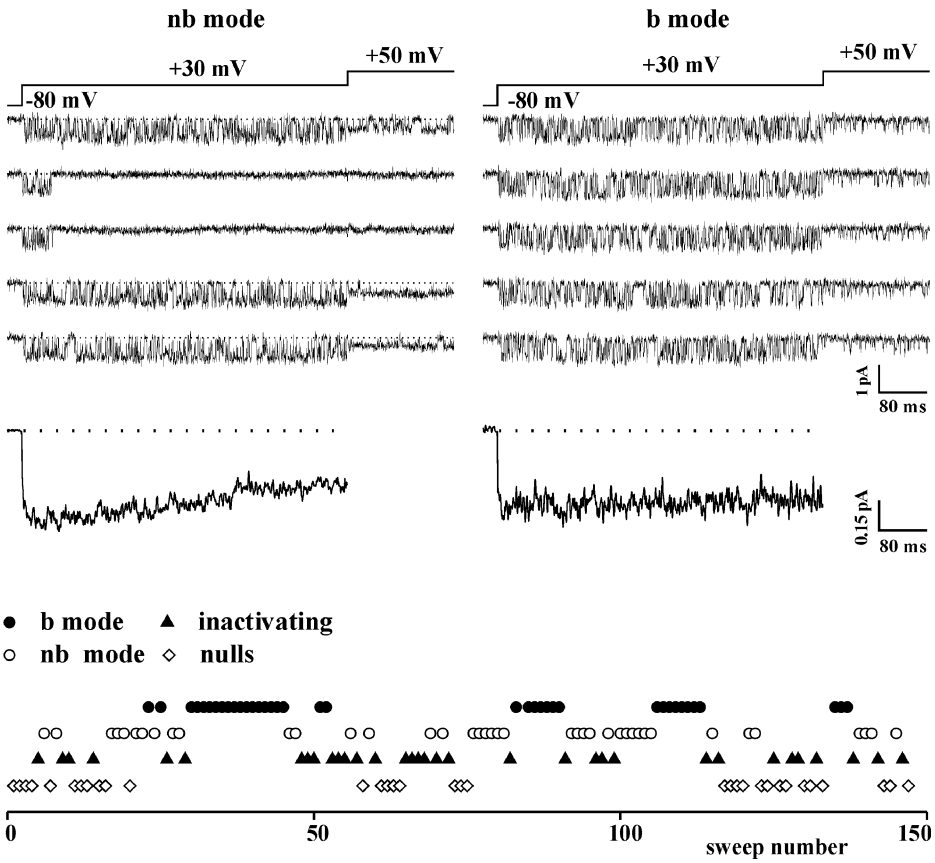

FIGURE 7. Switching between the b and nb gating modes produces reversible uncoupling of inactivation of $Ca_V2.1$ channels. Single channel recordings and voltage protocol as in Fig. 4. Representative current traces from a patch containing a single $Ca_V2.1$ channel in the fast gating mode showing frequent switching between the nb (left traces) and b (right traces) gating modes, as inferred from the gating pattern in the short pulse at +50 mV following the prepulse at +30 mV. Below the traces, the corresponding ensemble average currents at +30 mV for the nb (left, $n = 83$) and b (right, $n = 44$) gating modes are shown. Separate average currents for the b and nb gating modes at +30 mV were obtained considering the inactivating traces within a string of noninactivating sweeps showing b or nb mode activity as b or nb traces, respectively, and those at the beginning or at the end of an nb period as nb traces. The bottom panel shows the channel activity in consecutive sweeps, classified as b, nb, null, and inactivating. Note that channel inactivation at +30 mV occurs almost exclusively during periods with nb mode activity. The same is true for nulls; the probability that an nb sweep was preceded or followed by a null trace was 39/133 pairs = 0.28, whereas the probability that a b trace was preceded or followed by a null trace was 1/73 pairs = 0.014 (in this calculation, inactivating traces that were within and at the beginning or end of a string in nb mode were considered as nb sweeps).

+30 and +50 mV than that of N-type channels at +20 mV in Plummer and Hess, 1991), depolarizations much longer than those used in this report would be necessary to study (e.g., with run analysis) the temporal correlation between sweeps with inactivating (nb) and noninactivating (b) activity, as done in Plummer and Hess (1991).

Whereas some features of a channel in the b mode, such as the bell-shaped voltage dependence of the open probability and the shortening of the open times and lengthening of the closed dwell times with increasing voltage (at $V > 30$ mV), appear consistent with voltage-dependent open channel block by a cytoplasmic positively charged particle, the lack of inactivation and the increased availability of a channel in the b mode are not expected from a simple voltage-dependent open channel block. The possibility that open pore block by some cytoplasmic particle could itself somehow prevent the transition of the channel to an inactivated state can be excluded on the basis of the fact that uncoupling of inactivation also occurs at +30 mV, where there is no apparent pore block in the b mode. Hence, the name "blocked gating mode" seemed somewhat misleading and the name "b gating mode" seemed preferable. However, it remains possible that the low-po gating pattern observed at high voltages reflects the fact that an open channel in the noninactivating b mode can be reversibly blocked by a cytoplasmic positively charged particle, in contrast with a channel in the nb mode.

Reversible uncoupling of inactivation produced by switching between the nb and b gating modes, together with the high variability in the fraction of time spent in the b mode by individual channels in different single channel patches (0–90%), can explain the variability in both the kinetics of inactivation (at +30 mV) and the voltage dependence of steady-state inactivation observed for single $Ca_V2.1$ channels in either the fast or slow gating mode (Luvisetto et al., 2004). For example, the fraction of inactivating traces at +30 mV in 11 patches with a single $Ca_V2.1$ channel (containing the β_{2e} subunit) in the fast gating mode varied from 0 to 39% in different patches (average value 16 ± 5%), and steady-state inactivation at a holding potential of −20 mV ranged from complete to none (in six patches where the holding potential was varied, the average

open probability at −20 mV normalized to that at −80 mV was 0.68 ± 0.21). There appears to be a correlation between the fraction of inactivating traces or null traces and the fraction of time spent in the b gating mode by individual channels. In fact, in four patches containing a single $Ca_V2.1\alpha_1$–β_{2e}–$\alpha_{2b}\delta$-1 channel in the fast gating mode, where the b gating mode was either absent or rare, the average fraction of inactivating traces was 35 ± 1%, whereas in the other five patches, where 56 ± 9% of the traces at +40 and +50 mV showed b mode activity, the inactivating traces at +30 mV were only 6 ± 3%. Likewise, two single channels with no evidence of the b gating mode were completely inactivated at −20 mV, whereas three channels spending a large fraction of time in the b mode did not show any inactivation at −20 mV.

DISCUSSION

In this paper we show that human $Ca_V2.1$ channels in either the fast or slow gating mode (Luvisetto et al., 2004) can reversibly switch (in the time scale of seconds) to a noninactivating mode of gating, which we have called b mode. A channel in the b gating mode shows a bell-shaped voltage dependence of the open probability, with a characteristic low open probability at high positive voltages, decreasing with increasing voltage. Single $Ca_V2.1$ channels can then display four different modes of gating: fast-b, slow-b, fast-nb, and slow-nb (where nb refers to a mode in which the channel shows the usual voltage dependence of the open probability). At low voltages close to the threshold of channel activation, the mean open and closed times and the open probability of the channel in b gating modes (fast-b and slow-b) are similar to those of the channel in nb gating modes (fast-nb and slow-nb, respectively). At high voltages where the open probability of the channel in nb gating modes approaches its maximum value (V ≥ +40 mV with 90 mM Ba^{2+} as charge carrier), the channel in b gating modes has a much lower open probability and shorter mean open time. One can estimate that in physiological solutions, this would occur at V ≥ +10 mV, taking into account the change in surface potential caused by the high divalent ion concentration necessary to be able to resolve the very small unitary currents (Tottene et al., 2002). Therefore, Ca^{2+} influx in response to an action potential is expected to be different for $Ca_V2.1$ channels in b and nb gating modes (Sabatini and Regehr, 1999).

Perhaps the most striking feature of the $Ca_V.2.1$ channel in b gating modes (fast-b and slow-b) is the lack of inactivation during long pulses at high positive voltages, where the channel in nb gating modes (fast-nb and slow-nb) inactivates relatively rapidly. Moreover, the availability to open in response to a depolarization appears to be much larger for a $Ca_V.2.1$ channel in b gating modes (e.g., Fig. 7 and its legend). The switching between b and nb gating modes then produces a reversible uncoupling of inactivation of $Ca_V2.1$ channels, similar to that previously described for native N-type ($Ca_V2.2$) channels (Plummer and Hess, 1991). Single channel recordings of N-type channels at +20 mV (110 Ba^{2+}) revealed switching between an inactivating and a noninactivating gating mode with mean lifetimes of few seconds and similar open time distributions and first latency, as is the case for the $Ca_V2.1$ channel in b and nb gating modes at +20 mV. Gating of N-type channels at higher voltages was not studied by Plummer and Hess (1991). Later, Lee and Elmslie (1999) reported that at V ≥ +40 mV, N-type channels can display a low-p_o mode of gating with brief openings; no evidence for it was found at lower voltages, as expected if it corresponded to the b gating mode of $Ca_V2.1$ channels; however, its inactivation properties were not studied and no correlation was made with the noninactivating mode of the N-type channel described by Plummer and Hess (1991). We have provided evidence that the b gating mode underlies reversible uncoupling of inactivation of $Ca_V2.1$ channels, and suggest that a similar mode underlies reversible uncoupling of inactivation of $Ca_V2.2$ (N-type) channels.

The great impact that uncoupling from inactivation of $Ca_V2.1$ channels in the b gating mode may have on the magnitude and timing of Ca^{2+} influx in response to repetitive firing can be inferred by considering the Ca^{2+} current measured by Liu et al. (2003) during different types of physiologically relevant complex voltage waveforms, applied to different recombinant Ca_V channels and to $Ca_V2.1$ channels with distinct inactivation properties. The integrated Ca^{2+} current measured at physiological temperature during repetitive firing waveforms (containing both excitatory postsynaptic potentials and action potentials), which simulate the response of a pyramidal neuron to high-frequency (100 Hz) presynaptic stimulation, was almost 15 times larger for $Ca_V2.1$ channels with the β_{2a} subunit than for those with the β_{1b} subunit, as a consequence of the slower rate of inactivation and especially of the steady-state inactivation at more positive voltages of the channels containing the β_{2a} subunit. Given the lack of inactivation during long pulses and the increased steady-state availability of $Ca_V2.1$ channels in the b mode, one can predict that switching from the nb to the b gating mode would result in a large increase of Ca^{2+} influx through $Ca_V2.1$ channels during physiologically relevant repetitive firing waveforms. Most likely, the great enhancement of Ca^{2+} influx during repetitive firing, consequent to uncoupling from inactivation in the b mode, would prevail over the relatively small decrease of Ca^{2+} influx during a single action potential (consequent to the low open probability of $Ca_V2.1$ channels in the b

mode at high voltages). In fact, most of the Ca^{2+} influx during an action potential occurs during the repolarization phase (McCobb and Beam, 1991; Borst and Sakmann, 1998; Sabatini and Regehr, 1999; Bischofberger et al., 2002; Meinrenken et al., 2003), at voltages where the open probability is similar in the b and nb gating mode. Switching to the b mode would affect mainly Ca^{2+} entry at the peak of the action potential (and would perhaps alter mainly the timing of Ca^{2+} influx, reducing its duration) (Sabatini and Regehr, 1999).

As discussed in Luvisetto et al. (2004; see references therein), modal gating is widespread among channels, and regulation of the equilibrium between gating modes appears as a widespread mechanism for neuromodulation of channel function. $Ca_V2.1$ channels are known to be regulated by many different transmitters and various signaling pathways (Catterall, 2000; Dolphin, 2003; Elmslie, 2003). The mean lifetimes of the b and nb gating modes of $Ca_V2.1$ channels are compatible with a covalent reversible modification of the channel, such as phosphorylation. For L-type Ca^{2+} channels and M channels there are examples in the literature of gating mode switching in the time frame of seconds, where either the equilibrium between gating modes is modulated by phosphorylation/dephosphorylation reactions or the gating modes correspond to different states of phosphorylation of the channel (Ochi and Kawashima, 1990; Yue et al., 1990; Herzig et al., 1993; Ono and Fozzard, 1993; Marrion, 1996; Dzhura et al., 2000). However, in these cases, the gating modes had similar inactivation properties. Except for G proteins (Colecraft et al., 2001), modulation of $Ca_V2.1$ channels has not been studied at the single channel level. However, a shift in the equilibrium between b and nb gating modes may be possibly involved in the cAMP-dependent potentiation of $Ca_V2.1$ channels reported by Fukuda et al. (1996), since the potentiation was not seen at low voltages and was accompanied by an increased rate of inactivation of the whole-cell current. Moreover, a shift from the b to the nb mode consequent to channel phosphorylation may possibly underly the increased amplitude of the inactivating component of the N-type calcium current measured in sympathetic neurons upon dialysis with phosphatase inhibitors (Werz et al., 1993).

Assuming that a reversible covalent modification, such as phosphorylation, drives switching between b and nb modes, then the features of the b mode would be explained if the modification (e.g., channel dephosphorylation) both prevented inactivation and allowed voltage-dependent pore block by a cytoplasmic particle. Considering recent models of Ca^{2+} channel inactivation (Stotz et al., 2003; Kim et al., 2004), one may speculate that the modification that switches the channel to the b mode might prevent the physical occlusion of the pore by the intracellular domain I-II linker (the "hinged lid"), either hampering its movement or disrupting its docking site, likely formed by the innermost part of the S6 segments. In the latter hypothesis, a distortion of the four pore-forming S6 segments might also favor fast reversible open pore block by some unidentified cytoplasmic particle. The possibility that open pore block by this particle could itself somehow prevent the occlusion of the pore by the I-II linker can be excluded, because uncoupling of inactivation in the b mode also occurs at +30 mV, where there is no apparent pore block. An alternative possibility consistent with the data, is that voltage-dependent pore block is not involved in the b mode, and that the modification of the channel that prevents inactivation also confers anomalous gating properties to the $Ca_V2.1$ channel.

Regulation of the complex modal gating of $Ca_V2.1$ channels (described here and in Luvisetto et al., 2004) provides a potent and versatile mechanism to fine tune Ca^{2+} influx and Ca^{2+}-dependent processes to specific stimuli in a changing physiological environment. In many central synapses, $Ca_V2.1$ channels are preferentially located at the release sites and are more effectively coupled to neurotransmitter release than other Ca^{2+} channel types (Mintz et al., 1995; Wu et al., 1999; Qian and Noebels, 2001). At these synapses, the action potential–evoked Ca^{2+} influx and the local Ca^{2+} increase that triggers neurotransmitter release are mainly determined by the open probability, unitary conductance, and kinetics of opening and closing of $Ca_V2.1$ channels (Borst and Sakmann, 1998; Sabatini and Regehr, 1999; Bischofberger et al., 2002; Meinrenken et al., 2002, 2003). At some synapses, the inactivation properties of $Ca_V2.1$ channels may contribute to determine the time course of short-term synaptic plasticity, as shown for short-term depression at the Calyx of Held (Forsythe et al., 1998). Given the steep dependence of neurotransmitter release on Ca^{2+} influx (Dodge and Rahamimoff, 1967; Bollmann et al., 2000; Schneggenburger and Neher, 2000), any factor that modulates the equilibrium between the b and nb, and/or the fast and slow gating modes of $Ca_V2.1$ channels could be a potent regulator of both synaptic strength and synaptic plasticity. Switching to the b mode could decrease short-term depression by eliminating the contribution due to voltage-dependent $Ca_V2.1$ inactivation and also by decreasing the number of vesicles released per action potential, thus slowing down vesicle depletion. Switching to the slow mode would have a qualitatively similar effect, but mainly as a consequence of decreasing the release probability. Synaptic terminals of the same neurons may have different release probabilities and display short-term facilitation or depression depending on the target cell, most likely as a consequence of retrograde modulation by factors released

from the postsynaptic neuron (Atwood and Karunanithi, 2002). Modulation of presynaptic $Ca_V2.1$ channels might contribute to create diversity of release efficacy and short-term plasticity at different synapses; $Ca_V2.1$ channels in the slow-b mode would favor the synaptic phenotype of low release probability and short-term facilitation, whereas $Ca_V2.1$ channels in the fast-nb mode would favor the synaptic phenotype of high release probability and short-term depression. Thus, in general, regulation of the complex modal gating of $Ca_V2.1$ channels could have profound consequences on synaptic transmission and plasticity in the central nervous system.

$Ca_V2.1$ channels located in neuronal somatodendritic membranes are involved in regulating neural excitability, synaptic integration, and gene expression (Bayliss et al., 1997; Magee et al., 1998; Pineda et al., 1998; Sutton et al., 1999; Mori et al., 2000). As discussed above, switching of postsynaptic $Ca_V2.1$ channels to the noninactivating b mode could greatly increase Ca^{2+} entry during complex voltage waveforms, as those generated by a pyramidal neuron in response to high-frequency and theta rhythm presynaptic stimulation (Liu et al., 2003). Thus, regulation of modal gating of $Ca_V2.1$ channels could have profound consequences also on postsynaptic responses.

If, as it appears likely, the complex modal gating of $Ca_V2.1$ channels (described here and in Luvisetto et al., 2004) is associated with or modulated by chemical reactions and/or protein interactions, which may be different in different cells and/or different channel locations (c.f. the highly variable fraction of time spent by single $Ca_V2.1$ channels in each gating mode in any given patch), then differential modulation of the equilibrium between gating modes may contribute to generate the large functional diversity of native P/Q-type Ca^{2+} channels (Mintz et al., 1992; Usowicz et al., 1992; Randall and Tsien, 1995; Tottene et al., 1996; Forsythe et al., 1998; Mermelstein et al., 1999). Moreover, as discussed in Luvisetto et al. (2004), a variability in the equilibrium between gating modes likely accounts for the large variability in inactivation properties (both kinetics and voltage range of inactivation) of the whole-cell Ca^{2+} current, reported in both HEK293 cells and oocytes expressing $Ca_V2.1$ channels (Moreno et al., 1997; Restituito et al., 2001; Rousset et al., 2001), and probably also for the similar variability noted in tsA201cells expressing $Ca_V2.2$ channels (Hurley et al., 2000).

We thank Mark Williams (Merck Research Labs, San Diego, CA) for the human $\alpha_{1A\text{-}2}$, $\alpha_{2b}\delta$-1, and β_{1b} cDNAs and the A68-90 cell line.

The financial support of Telethon-Italy and the Italian Ministry of Education University Research (PRIN, FIRB, ST-L.449/97-CNR-MIUR, FISR-L.16/10/2000-CNR-MIUR) to Daniela Pietrobon is gratefully acknowledged.

Olaf S. Andersen served as editor.

Submitted: 3 February 2004
Accepted: 17 September 2004

REFERENCES

Atwood, H.L., and S. Karunanithi. 2002. Diversification of synaptic strength: presynaptic elements. *Nat. Rev. Neurosci.* 3:497–516.

Bayliss, D.A., Y.W. Li, and E.M. Talley. 1997. Effects of serotonin on caudal raphe neurons: inhibition of N- and P/Q-type calcium channels and the afterhyperpolarization. *J. Neurophysiol.* 77:1362–1374.

Bischofberger, J., J.R. Geiger, and P. Jonas. 2002. Timing and efficacy of Ca^{2+} channel activation in hippocampal mossy fiber boutons. *J. Neurosci.* 22:10593–10602.

Bollmann, J.H., B. Sakmann, and J.G. Borst. 2000. Calcium sensitivity of glutamate release in a calyx-type terminal. *Science.* 289:953–957.

Borst, J.G., and B. Sakmann. 1998. Facilitation of presynaptic calcium currents in the rat brainstem. *J. Physiol.* 513:149–155.

Catterall, W.A. 2000. Structure and regulation of voltage-gated Ca^{2+} channels. *Annu. Rev. Cell Dev. Biol.* 16:521–555.

Colecraft, H.M., D.L. Brody, and D.T. Yue. 2001. G-protein inhibition of N- and P/Q-type calcium channels: distinctive elementary mechanisms and their functional impact. *J. Neurosci.* 21:1137–1147.

Dodge, F.A., Jr., and R. Rahamimoff. 1967. Co-operative action of calcium ions in transmitter release at the neuromuscular junction. *J. Physiol.* 193:419–432.

Dolphin, A.C. 2003. G protein modulation of voltage-gated calcium channels. *Pharmacol. Rev.* 55:607–627.

Dunlap, K., J.I. Luebke, and T.J. Turner. 1995. Exocytotic Ca^{2+} channels in mammalian central neurons. *Trends Neurosci.* 18:89–98.

Dzhura, I., Y. Wu, R.J. Colbran, J.R. Balser, and M.E. Anderson. 2000. Calmodulin kinase determines calcium-dependent facilitation of L-type calcium channels. *Nat. Cell Biol.* 2:173–177.

Elmslie, K.S. 2003. Neurotransmitter modulation of neuronal calcium channels. *J. Bioenerg. Biomembr.* 35:477–489.

Forsythe, I.D., T. Tsujimoto, M. Barnes-Davies, M.F. Cuttle, and T. Takahashi. 1998. Inactivation of presynaptic calcium current contributes to synaptic depression at a fast central synapse. *Neuron.* 20:797–807.

Fukuda, K., S. Kaneko, N. Yada, M. Kikuwaka, A. Akaike, and M. Satoh. 1996. Cyclic AMP-dependent modulation of N- and Q-type Ca^{2+} channels expressed in *Xenopus* oocytes. *Neurosci. Lett.* 217: 13–16.

Hans, M., S. Luvisetto, M.E. Williams, M. Spagnolo, A. Urrutia, A. Tottene, P.F. Brust, E.C. Johnson, M.M. Harpold, K.A. Stauderman, and D. Pietrobon. 1999. Functional consequences of mutations in the human α1A calcium channel subunit linked to familial hemiplegic migraine. *J. Neurosci.* 19:1610–1619.

Herzig, S., P. Patil, J. Neumann, C.M. Staschen, and D.T. Yue. 1993. Mechanisms of β-adrenergic stimulation of cardiac Ca^{2+} channels revealed by discrete-time Markov analysis of slow gating. *Biophys. J.* 65:1599–1612.

Horn, R., C.A. Vandenberg, and K. Lange. 1984. Statistical analysis of single sodium channels. Effects of N-bromoacetamide. *Biophys. J.* 45:323–335.

Hurley, J.H., A.L. Cahill, K.P. Currie, and A.P. Fox. 2000. The role of dynamic palmitoylation in Ca^{2+} channel inactivation. *Proc. Natl. Acad. Sci. USA.* 97:9293–9298.

Kim, J., S. Ghosh, D.A. Nunziato, and G.S. Pitt. 2004. Identification of the components controlling inactivation of voltage-gated Ca^{2+} channels. *Neuron.* 41:745–754.

Lee, H.K., and K.S. Elmslie. 1999. Gating of single N-type calcium channels recorded from bullfrog sympathetic neurons. *J. Gen. Physiol.* 113:111–124.

Liu, Z., J. Ren, and T.H. Murphy. 2003. Decoding of synaptic voltage waveforms by specific classes of recombinant high-threshold Ca^{2+} channels. *J. Physiol.* 553:473–488.

Luvisetto, S., T. Fellin, M. Spagnolo, B. Hivert, P.F. Brust, M.M. Harpold, K.A. Stauderman, M.E. Williams, and D. Pietrobon. 2004. Modal gating of human $Ca_V2.1$ (P/Q-type) calcium channels: I. the slow and the fast gating modes and their modulation by β subunits. *J. Gen. Physiol.* 124:445–461.

Magee, J., D. Hoffman, C. Colbert, and D. Johnston. 1998. Electrical and calcium signaling in dendrites of hippocampal pyramidal neurons. *Annu. Rev. Physiol.* 60:327–346.

Marrion, N.V. 1996. Calcineurin regulates M channel modal gating in sympathetic neurons. *Neuron.* 16:163–173.

McCobb, D.P., and K.G. Beam. 1991. Action potential waveform voltage-clamp commands reveal striking differences in calcium entry via low and high voltage-activated calcium channels. *Neuron.* 7:119–127.

Meinrenken, C.J., J.G. Borst, and B. Sakmann. 2002. Calcium secretion coupling at calyx of held governed by nonuniform channel-vesicle topography. *J. Neurosci.* 22:1648–1667.

Meinrenken, C.J., J.G. Borst, and B. Sakmann. 2003. Local routes revisited: the space and time dependence of the Ca^{2+} signal for phasic transmitter release at the rat calyx of Held. *J. Physiol.* 547: 665–689.

Mermelstein, P.G., R.C. Foehring, T. Tkatch, W.J. Song, G. Baranauskas, and D.J. Surmeier. 1999. Properties of Q-type calcium channels in neostriatal and cortical neurons are correlated with β subunit expression. *J. Neurosci.* 19:7268–7277.

Mintz, I.M., B.L. Sabatini, and W.G. Regehr. 1995. Calcium control of transmitter release at a cerebellar synapse. *Neuron.* 15:675–688.

Mintz, I.M., V.J. Venema, K.M. Swiderek, T.D. Lee, B.P. Bean, and M.E. Adams. 1992. P-type calcium channels blocked by the spider toxin ω-Aga-IVA. *Nature.* 355:827–829.

Moreno, H., B. Rudy, and R. Llinas. 1997. β subunits influence the biophysical and pharmacological differences between P- and Q-type calcium currents expressed in a mammalian cell line. *Proc. Natl. Acad. Sci. USA.* 94:14042–14047.

Mori, Y., M. Wakamori, S. Oda, C.F. Fletcher, N. Sekiguchi, E. Mori, N.G. Copeland, N.A. Jenkins, K. Matsushita, Z. Matsuyama, and K. Imoto. 2000. Reduced voltage sensitivity of activation of P/Q-type Ca^{2+} channels is associated with the ataxic mouse mutation rolling Nagoya (tg(rol)). *J. Neurosci.* 20:5654–5662.

Nilius, B. 1988. Modal gating behavior of cardiac sodium channels in cell-free membrane patches. *Biophys. J.* 53:857–862.

Ochi, R., and Y. Kawashima. 1990. Modulation of slow gating process of calcium channels by isoprenaline in guinea-pig ventricular cells. *J. Physiol.* 424:187–204.

Ono, K., and H.A. Fozzard. 1993. Two phosphatase sites on the Ca^{2+} channel affecting different kinetic functions. *J. Physiol.* 470: 73–84.

Pineda, J.C., R.S. Waters, and R.C. Foehring. 1998. Specificity in the interaction of HVA Ca^{2+} channel types with Ca^{2+}-dependent AHPs and firing behavior in neocortical pyramidal neurons. *J. Neurophysiol.* 79:2522–2534.

Plummer, M.R., and P. Hess. 1991. Reversible uncoupling of inactivation in N-type calcium channels. *Nature.* 351:657–659.

Qian, J., and J.L. Noebels. 2001. Presynaptic Ca^{2+} channels and neurotransmitter release at the terminal of a mouse cortical neuron. *J. Neurosci.* 21:3721–3728.

Randall, A., and R.W. Tsien. 1995. Pharmacological dissection of multiple types of Ca^{2+} channel currents in rat cerebellar granule neurons. *J. Neurosci.* 15:2995–3012.

Restituito, S., T. Cens, M. Rousset, and P. Charnet. 2001. Ca^{2+} channel inactivation heterogeneity reveals physiological unbinding of auxiliary β subunits. *Biophys. J.* 81:89–96.

Rousset, M., T. Cens, S. Restituito, C. Barrere, J.L. Black III, M.W. McEnery, and P. Charnet. 2001. Functional roles of γ2, γ3, and γ4, three new Ca^{2+} channel subunits, in P/Q-type Ca^{2+} channel expressed in *Xenopus* oocytes. *J. Physiol.* 532:583–593.

Sabatini, B.L., and W.G. Regehr. 1999. Timing of synaptic transmission. *Annu. Rev. Physiol.* 61:521–542.

Schneggenburger, R., and E. Neher. 2000. Intracellular calcium dependence of transmitter release rates at a fast central synapse. *Nature.* 406:889–893.

Stotz, S.C., E.J. Jarvis, and G.W. Zamponi. 2003. Functional roles of cytoplasmic loops and pore lining transmembrane helices in the voltage-dependent inactivation of HVA calcium channels. *J. Physiol.* 554:263–273.

Sutton, K.G., J.E. McRory, H. Guthrie, T.H. Murphy, and T.P. Snutch. 1999. P/Q-type calcium channels mediate the activity-dependent feedback of syntaxin-1A. *Nature.* 401:800–804.

Tottene, A., T. Fellin, S. Pagnutti, S. Luvisetto, J. Striessnig, C. Fletcher, and D. Pietrobon. 2002. Familial hemiplegic migraine mutations increase Ca^{2+} influx through single human $Ca_V2.1$ channels and decrease maximal $Ca_V2.1$ current density in neurons. *Proc. Natl. Acad. Sci. USA.* 99:13284–13289.

Tottene, A., A. Moretti, and D. Pietrobon. 1996. Functional diversity of P-type and R-type calcium channels in rat cerebellar neurons. *J. Neurosci.* 16:6353–6363.

Usowicz, M.M., M. Sugimori, B. Cherksey, and R. Llinas. 1992. P-type calcium channels in the somata and dendrites of adult cerebellar Purkinje cells. *Neuron.* 9:1185–1199.

van den Maagdenberg, A.M., D. Pietrobon, T. Pizzorusso, S. Kaja, L.A. Broos, T. Cesetti, R.C. van de Ven, A. Tottene, J. van der Kaa, J.J. Plomp, et al. 2004. Cacna1a knockin migraine mouse model with increased susceptibility to cortical spreading depression. *Neuron.* 41:701–710.

Werz, M.A., K.S. Elmslie, and S.W. Jones. 1993. Phosphorylation enhances inactivation of N-type calcium channel current in bullfrog sympathetic neurons. *Pflugers Arch.* 424:538–545.

Wu, L.G., R.E. Westenbroek, J.G. Borst, W.A. Catterall, and B. Sakmann. 1999. Calcium channel types with distinct presynaptic localization couple differentially to transmitter release in single calyx-type synapses. *J. Neurosci.* 19:726–736.

Yue, D.T., P.H. Backx, and J.P. Imredy. 1990. Calcium-sensitive inactivation in the gating of single calcium channels. *Science.* 250: 1735–1738.